Ferromagnetic Coupling of Mononuclear Fe Centers in a Self-Assembled Metal-Organic Network on Au(111)

T. R. Umbach,[1] M. Bernien,[1] C. F. Hermanns,[1] A. Krüger,[1] V. Sessi,[2] I. Fernandez-Torrente,[1] P. Stoll,[1,3] J. I. Pascual,[1,3,4] K. J. Franke,[1,3,5] and W. Kuch[1,3]

[1]*Freie Universität Berlin, Fachbereich Physik, Arnimallee 14, 14195 Berlin, Germany*
[2]*European Synchrotron Radiation Facility, PB 220, 38043 Grenoble, France*
[3]*Center for Supramolecular Interactions, Freie Universität Berlin, Arnimallee 14, 14195 Berlin, Germany*
[4]*CIC nanoGUNE, 20018 Donostia-San Sebastian, Spain, and Ikerbasque, Basque Foundation for Science, 48011 Bilbao, Spain*
[5]*Institut für Festkörperphysik, Technische Universität Berlin, Hardenbergstraße 36, 10623 Berlin, Germany*

(Received 27 August 2012; published 26 December 2012)

The magnetic state and magnetic coupling of individual atoms in nanoscale structures relies on a delicate balance between different interactions with the atomic-scale surroundings. Using scanning tunneling microscopy, we resolve the self-assembled formation of highly ordered bilayer structures of Fe atoms and organic linker molecules (T4PT) when deposited on a Au(111) surface. The Fe atoms are encaged in a three-dimensional coordination motif by three T4PT molecules in the surface plane and an additional T4PT unit on top. Within this crystal field, the Fe atoms retain a magnetic ground state with easy-axis anisotropy, as evidenced by x-ray absorption spectroscopy and x-ray magnetic circular dichroism. The magnetization curves reveal the existence of ferromagnetic coupling between the Fe centers.

DOI: 10.1103/PhysRevLett.109.267207 PACS numbers: 75.70.−i, 68.37.Ef, 75.30.Et, 78.70.Dm

As the size of a magnetic material decreases, the stability of the collective magnetic ground state becomes weaker, leading to paramagnetic behavior at atomic-scale dimensions [1]. The identification and study of mechanisms for stabilizing magnetically oriented ground states aims to provide routes for the design and construction of nanomaterials (clusters and thin films) that retain some magnetic order at temperatures as high as possible. At the limit of individual atoms deposited on a metal surface, magnetic anisotropy and interatomic coupling are the key ingredients to tune the magnetism of a nanostructure [2]. The anisotropy of the atomic environment may lower the magnetic moment but, in turn, defines easy directions for magnetization. Exchange interactions coupling the magnetic moment of neighbor atoms drive the formation of magnetically ordered states, but this effect quickly vanishes with increasing interatomic distance. Only the indirect exchange coupling through valence electrons of the metal support (the Ruderman-Kittel-Kasuya-Yosida (RKKY) interaction [3–7]) may be operative. It has been shown that RKKY interactions lead to collective ferromagnetic or antiferromagnetic ground states, but the exchange energy is small ($J \sim 50$ μeV) [1,7,8].

An interesting approach to enhance the magnetic anisotropy of atoms in a thin film is to augment the ligand field splitting of the d levels by coordination to specifically selected organic ligands [2]. The formation of a coordination bond to molecular end groups induces a charge redistribution at the metal sites and casts the ligand field by adopting high-symmetry metal-organic structures and periodic networks [9–11]. In bulk metal-organic materials, the organic linkers connecting magnetic metal centers also mediate the magnetic coupling between them by means of electronic states extended along the organic backbone [12,13]. The presence of such a superexchange mechanism for magnetic coupling in metal-organic thin films could optimize the stabilization of collective magnetic ground states, but its detection still remains a challenge.

Here, we show the existence of ferromagnetic coupling between Fe ions within a self-assembled metal-organic film grown on a Au(111) surface. Single Fe atoms lie in three-dimensional coordination sites and are connected to neighboring Fe atoms by 2,4,6-tris(4-pyridyl)-1,3,5-triazine (T4PT) molecules [see Fig. 1(b)]. Analysis of x-ray

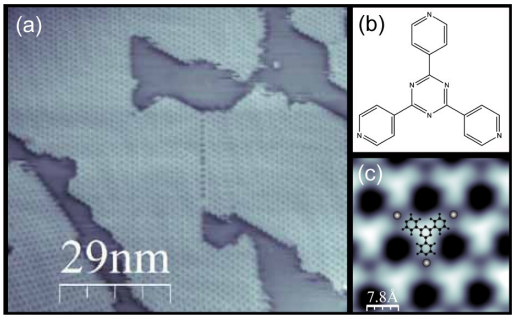

FIG. 1 (color online). (a) Large-scale STM topography image of the coordinated Fe-T4PT islands on the Au(111) surface ($I = 253$ pA, $V_S = -1.5$ V). The Fe-T4PT islands are homogeneous over the whole surface. There is no indication of Fe clusters. The STM image was obtained with a room-temperature STM at the ID08 beam line at the ESRF directly before x-ray investigations. (b) Molecular structure of T4PT. (c) An STM zoom evidences the metal coordination of the T4PT molecules ($I = 230$ pA, $V_S = 0.06$ V). STM image processing by WSXM [39].

absorption spectroscopy (XAS) and x-ray magnetic circular dichroism (XMCD) measurements reveals a high spin $S = 2$ ground state with an out-of-plane magnetic anisotropy. Magnetization curves of the ultrathin layer exhibit deviations from the case of noninteracting paramagnetic moments, which are interpreted as a finite ferromagnetic interaction between the mononuclear centers on the basis of a mean-field model.

Fe-T4PT networks were grown on an atomically clean Au(111) single crystal. The gold surface was first precovered at room temperature by a submonolayer amount of T4PT molecules, sublimated from a Knudsen cell, and by Fe atoms. Subsequently, the substrate was annealed to 400 K to activate the formation of coordination bonds. The structure of the resulting surface was characterized *in situ*, in our low temperature (4.8 K) scanning tunneling microscope (STM). XAS and XMCD measurements in total electron yield were performed at the beam line ID08 at the European Synchrotron Radiation Facility (ESRF). The beam size on the sample was about 1.4 mm (FWHM) in the horizontal and 50 μm in the vertical direction. The sample was kept at a temperature of 8 K in a variable external magnetic field up to 5 T and exposed to x-rays under different incidence angles. Here, STM measurements (Fig. 1) were carried out *in situ* at several macroscopically separated areas, indicating that the sample was covered by a homogeneous metal-organic network and that there are no uncoordinated Fe clusters.

Large-scale STM images show the tendency of Fe atoms and T4PT molecules to coordinate in networks with a high degree of order [Fig. 1(a)]. The presence of the Au(111) herringbone reconstruction underneath the metal-organic layer indicates a weak interaction with the substrate. STM images recorded at low bias voltage ($V_S < 0.5$ V) resolve the skeleton of the T4PT molecules [Fig. 1(c)]. Each pyridyl group participates in a threefold node, a configuration that can only be stable if the natural repulsion between electrophilic end groups is overcome by insertion of a bonding center prone to coordinate with the N lone-pair electrons [9,11]. Hence, we anticipate the inclusion of Fe atoms at these sites [14].

The structure of the Fe-T4PT network shows a peculiar dependence on the bias voltage applied during its inspection [Figs. 2(a) and 2(b)]. Starting from the low bias voltage structure in Fig. 2(a), an increase of the sample bias voltage above 0.6 V results in the observation of a new set of T4PT molecules centered on the Fe sites and rotated by $\varphi = 29°$ [Fig. 2(b)]. These new features can not be associated to tunneling through different orbitals of the same molecules due to their different orientation. Furthermore, we observe domains with mirror symmetry around dislocation lines at high bias voltage that are absent when inspected at low bias voltage (see Supplemental Material S1 [15]). On the basis of these facts, we conclude that the film consists of a bilayer of T4PT molecules: Fe atoms coordinate to the pyridyl

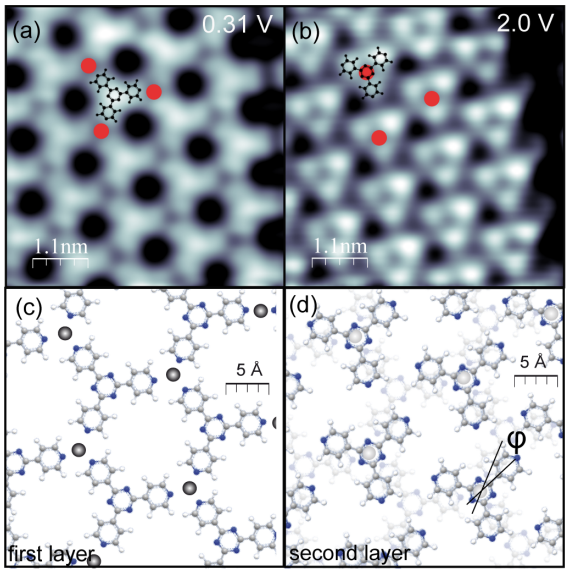

FIG. 2 (color online). [(a) and (b)] STM images of an Fe-T4PT network measured at different sample bias voltages ($I = 0.33$ nA, (a) $V_S = 0.31$ V, (b) $V_S = 2.0$ V). (c) Structure of the first layer of the Fe-T4PT network. Fe atoms are threefold coordinated by three T4PT molecules in the first layer. (d) In the second layer, T4PT molecules are centered at the Fe sites and are rotated by $\varphi = 29°$ with respect to the first-layer molecules (indicated by the black lines).

groups of three T4PT molecules in the bottom layer [first layer in Fig. 2(c)] and to the triazine center of an additional T4PT molecule directly on top [second layer in Fig. 2(d)]. Their different aspect with the bias voltage can be rationalized by considering that the top layer is only weakly coupled to the metallic substrate and poorly screened [16]. Its electronic gap becomes wider and the molecule is then more transparent to electrons tunneling close to the Fermi level E_F [17,18], allowing us to resolve the structure of the bottom layer at low bias voltages.

In the resulting structure, the Fe atom is located in a three-dimensional coordination cavity, encaged by a total of six nitrogen atoms [Figs. 2(c) and 2(d)]. The presence of the top T4PT molecule centered directly on Fe sites suggests that the triazine moiety also participates in the coordination with the metal atom. A probable scenario is that this metal-ligand bond causes an upward displacement of the Fe atom [11,19,20], which would cause a distortion of the ligand field around the Fe atom, bringing it from a trigonal-planar into a three-dimensional (pyramidal) structure [21,22]. This configuration could help to prevent the quenching of its magnetic moment due to the interaction with the gold surface.

To investigate the magnetic properties of the Fe atoms in the Fe-T4PT networks, we have performed XAS and XMCD measurements at $T = 8$ K in an applied magnetic field of 5 T (Fig. 3). From the line shape and position of the XAS L_3 peak [Fig. 3(a), maximum at 707.2 eV], we conclude that we probe isolated Fe atoms in a +2 oxidation state [23,26–28] [the spectrum clearly deviates from that of Fe(III), shown with a

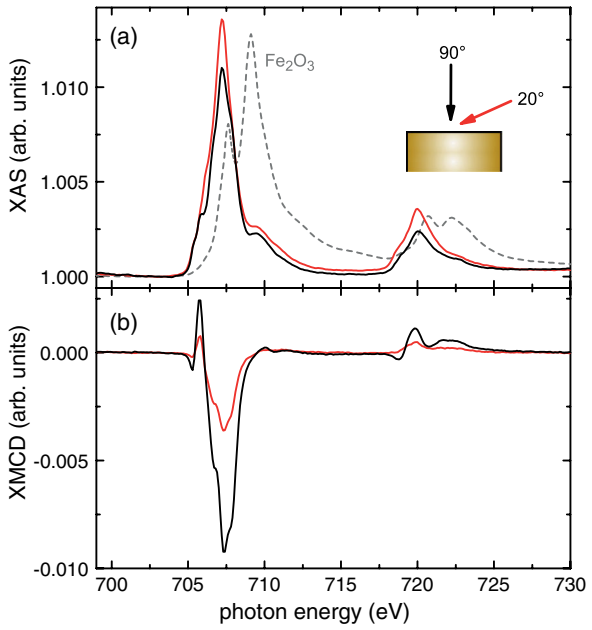

FIG. 3 (color online). (a) XAS and (b) XMCD difference spectra at the Fe $L_{2,3}$ edges of Fe-T4PT on Au(111), measured at a temperature of 8 K in an applied magnetic field of 5 T for two different angles of incidence, as defined in the sketch in the top panel. The magnetic field was always parallel to the x-ray beam. The dashed line represents an XAS spectrum of the $L_{2,3}$ edge in Fe_2O_3, where Fe is in a +3 oxidation state. The shift of the absorption edge is due to the chemical sensitivity of the binding energy of the core-level electrons.

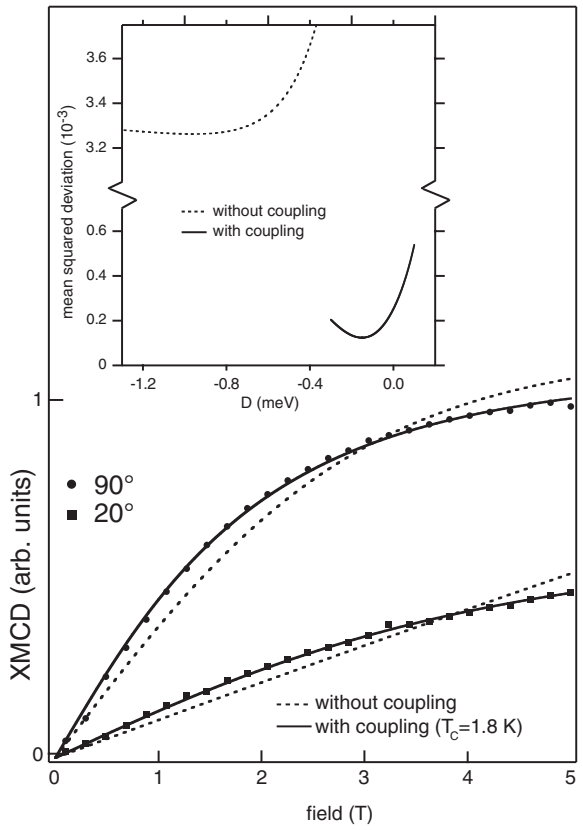

FIG. 4. Magnetic field dependence of the XMCD at the Fe L_3 edge of Fe-T4PT on Au(111) for x-ray incidence normal to the surface (circles) and at 20° grazing incidence (squares), measured at a temperature of 8 K. The magnetic field was always parallel to the x-ray beam. Dashed lines are the best fits of a paramagnetic spin Hamiltonian for $S = 2$, $T = 8$ K, and $D = -1.16$ meV; solid lines are the result of a simulation using mean-field-coupled magnetic moments with $T_C = 1.8$ K (see text). The inset shows the mean squared deviation between the experimental field dependence of XMCD data and the simulation by the paramagnetic spin Hamiltonian (dashed line) and the mean-field model, as described in the main text, as a function of the anisotropy, represented by the zero-field splitting parameter D. For each value of D, all other fit parameters have been optimized.

dashed line in Fig. 3(a) for comparison]. A +2 oxidation state is typical in bulk mononuclear iron complexes [22], thus supporting the three-dimensional coordination motif described in Fig. 2(d). Multiplet calculations of the XAS and XMCD difference spectra indicate an $S = 2$ high-spin state (see Supplemental Material S2 [15]).

The presence of a magnetic moment is further corroborated by XMCD spectra shown in Fig. 3(b). The XMCD difference signal of the L_3 peak exhibits a characteristic dip-peak structure at the low-energy side. While the line shapes are similar for different angles of incidence, there is a large change in the XMCD peak height: the signal at normal incidence is more than a factor of 2 higher than that at grazing incidence (20°). The higher XMCD signal in normal incidence points towards an easy-axis magnetic anisotropy along the direction normal to the surface, which is a result of the spin-orbit-induced mixing of nearly degenerate Fe 3d levels in the surrounding ligand field.

Figure 4 shows the evolution of the Fe L_3 XMCD signal with applied external magnetic field for both perpendicular and grazing incidence. The curvature of these plots allows us to quantify the anisotropy of the system. We start first by simulating the magnetization curves assuming noninteracting paramagnetic moments under the presence of magnetic anisotropy by means of a spin Hamiltonian approach:

$$\mathcal{H} = DS_z^2 - \mu_B g \mathbf{B}\cdot\mathbf{S}. \quad (1)$$

The first term describes the anisotropy energy through the zero-field-splitting parameter D and S_z, the spin component normal to the molecular plane (a negative D stands for an easy axis along z). The second term accounts for the Zeeman energy ($\mathbf{S}$ is the spin vector, $\mathbf{B}$ is the vector of the external field, μ_B is Bohr's magneton, and we consider a g factor of 2). Solving Eq. (1) for the two directions of measurement and calculating the magnetization from the thermal population of the resulting levels allows us to simulate magnetization plots as in Fig. 4 for several conditions. The curvature of the magnetization plots is an expression of the anisotropy of the system and can be

tuned by adjusting the parameter D. The larger curvature in normal incidence corroborates that this direction is the easy axis for magnetization ($D < 0$). However, the experimental curvature cannot be properly reproduced, no matter what value of D is used. The dashed line in the inset of Fig. 4 shows the mean squared deviation between experiment and simulations evaluating Eq. (1) as a function of D. We obtain large standard deviations for all values of D, even when the curvature is simulated using unrealistically high D values. We thus conclude that the experimental data are not compatible with noninteracting anisotropic paramagnetic moments but bear instead evidence for a magnetic coupling between neighboring Fe moments [29].

To include magnetic interactions between nearest neighbors, we resort to a mean-field description to simulate the magnetization curves. In this model, the magnetic interaction of a spin with all other spins in the neighborhood is replaced by an effective mean magnetic field added to the external applied field and proportional to the magnetization of the ensemble with proportionality factor $T_C = \sum_i J_i/(3k_B)$. Here, J_i is a Heisenberg-type interaction of the spin with a spin at site i and k_B is the Boltzmann constant. The sum goes over all sites with nonvanishing J_i. T_C represents the Curie temperature in the limit of vanishing anisotropy.

The solid lines in Fig. 4 are the result of such a simulation with $D = -0.35$ meV and $T_C = 1.8$ K. These values correspond to a global minimum (see solid line in the inset of Fig. 4 and Supplemental Material S4 [15]), reproducing correctly the experimental magnetization curves. While the model may not capture the details of the coupling mechanism, it clearly evidences the necessity to include ferromagnetic coupling of the Fe atoms to explain the experimental curves. If we assume a coupling to only the six nearest neighbor Fe atoms, the coupling constant $J_i = k_B T_C/2$ has to be on the order of ≈ 80 μeV to reproduce the experimentally observed magnetization curves [31]. Since the measurements are carried out well above T_C, the effect of correlated fluctuations, which would lead to an underestimation of the derived coupling strength in the mean-field description, is small.

Due to the relatively large distance between the Fe centers ($r = 1.3$ nm), a direct exchange coupling is very unlikely to be the origin of the observed ferromagnetic coupling. An indirect coupling mechanism via the polarization of the surface and bulk conduction electrons has been shown to exist on metal surfaces [6,7,32,33]. The RKKY interaction exhibits an oscillating ferromagnetic-antiferromagnetic coupling with the distance r of the magnetic moments. It can be described as $J_{\mathrm{RKKY}} \propto [\cos(2k_F r)]/(2k_F r)^d$ [7,34], where k_F is the Fermi wave vector and d defines the dimensionality of the conduction electron system. The Fermi wave vector of the Rashba-split surface state amounts to $k_{F,1} \approx 1.7$ nm [35]. Hence, a pairwise interaction of the Fe atoms at a distance of 1.3 nm via RKKY interactions would result in a weakly coupled antiferromagnetic ground state. Furthermore, we expect that the sixfold ligated Fe atoms are lifted from the surface [19,20] and thus only interact weakly with the substrate electrons. Despite small effects that may change the scattering phase shift of the conduction electrons, we may tentatively exclude a significant contribution of an RKKY-mediated coupling.

The molecular ligands coordinated to two neighbor Fe atoms can also play an important role in mediating magnetic interactions through a superexchange mechanism. Ferromagnetic and antiferromagnetic exchange interactions in metal-organic frameworks are well-known in bulk materials [12] for nitrogen-based organic linkers and transition-metal atoms. The superexchange mechanism is enhanced when conjugated molecular states bridge the magnetic centers [36], as is the case for Fe-T4PT networks. The spin polarization qualitatively follows a simple alternation rule: an even number of linker atoms in the pathway leads to antiferromagnetic coupling, whereas an odd number results in ferromagnetic coupling. In the case of the Fe-T4PT network, the alternation rule results in a ferromagnetic coupling between neighboring Fe centers. This is consistent with the positive (ferromagnetic) Heisenberg-type interaction J_i deduced from the magnetization curves.

Our results clearly sustain the presence of ferromagnetic coupling of Fe atoms connected by organic molecules in a highly ordered metal-organic network. The peculiarity of the observed network is that it consists of a bilayer structure, in which the Fe is coordinated by three pyridyl groups and one triazine unit. The central triazine ligand may further be responsible for a lifting of the Fe atoms from the metallic surface due to the trans effect [19,20]. This configuration eases the formation of a $+2$ oxidation state with a net spin. The resulting magnetic moments of the Fe ions are coupled ferromagnetically with each other, probably via a superexchange mechanism mediated by the organic linkers. These results further demonstrate that magnetism in two-dimensional metal-organic networks on a metal surface is feasible without the use of ferromagnetic substrates and suggests a route to engineer its magnetic character by enclosing the magnetic centers in self-assembled three-dimensional coordination cavities. To increase the stability of such magnetic networks for potential applications, a larger anisotropy and significantly stronger magnetic coupling strengths are required. Chemical design strategies toward this goal may comprise the use of radical ligands, known from bulk metal-organic ferromagnetic materials [37,38].

We thank Hendrik Mohrmann for fruitful discussions. We also acknowledge financial support by the Deutsche Forschungsgemeinschaft [(Grant No. FR 2726/1 and collaborative research center (Sfb 658)] and by the Center for Supramolecular Interactions (CSI) of the Freie Universität Berlin.

[1] S. Loth, S. Baumann, C. P. Lutz, D. M. Eigler, and A. J. Heinrich, Science **335**, 196 (2012).
[2] P. Gambardella *et al.*, Nat. Mater. **8**, 189 (2009).
[3] M. A. Ruderman and C. Kittel, Phys. Rev. **96**, 99 (1954).
[4] T. Kasuya, Prog. Theor. Phys. **16**, 45 (1956).
[5] K. Yosida, Phys. Rev. **106**, 893 (1957).
[6] P. Wahl, P. Simon, L. Diekhoner, V. S. Stepanyuk, P. Bruno, M. A. Schneider, and K. Kern, Phys. Rev. Lett. **98**, 056601 (2007).
[7] F. Meier, L. Zhou, J. Wiebe, and R. Wiesendanger, Science **320**, 82 (2008).
[8] A. A. Khajetoorians, J. Wiebe, B. Chilian, S. Lounis, S. Blügel, and R. Wiesendanger, Nat. Phys. **8**, 497 (2012).
[9] U. Schlickum *et al.*, Nano Lett. **7**, 3813 (2007).
[10] J. V. Barth, Surf. Sci. **603**, 1533 (2009).
[11] N. Henningsen, R. Rurali, R. Limbach, C. Drost, J. Pascual, and K. J. Franke, J. Phys. Chem. Lett. **2**, 55 (2011).
[12] J. A. McCleverty and M. D. Ward, Acc. Chem. Res. **31**, 842 (1998).
[13] W. Wernsdorfer, N. Aliaga-Alcalde, D. N. Hendrickson, and G. Christou, Nature (London) **416**, 406 (2002).
[14] Growth of T4PT films without deposition of Fe atoms resulted in a completely different layer structure, where direct bonds between N atoms of pyridyl moieties are fully absent.
[15] See Supplemental Material at http://link.aps.org/supplemental/10.1103/PhysRevLett.109.267207 for details of the bias voltage dependence of STM images, multiplet calculations of the x-ray absorption at the Fe $L_{2,3}$ edge, a description of the fit of the magnetization curves and its error margins, and a discussion of the spin state of the Fe ions.
[16] I. Fernandez-Torrente, K. J. Franke, and J. I. Pascual, J. Phys. Condens. Matter **20**, 184001 (2008).
[17] J. Repp, G. Meyer, S. M. Stojković, A. Gourdon, and C. Joachim, Phys. Rev. Lett. **94**, 026803 (2005).
[18] M. Takada and H. Tada, Chem. Phys. Lett. **392**, 265 (2004).
[19] K. Flechtner, A. Kretschmann, H.-P. Steinrück, and J. M. Gottfried, J. Am. Chem. Soc. **129**, 12110 (2007).
[20] C. Isvoranu, J. Knudsen, E. Ataman, K. Schulte, B. Wang, M.-L. Bocquet, J. N. Andersen, and J. Schnadt, J. Chem. Phys. **134**, 114711 (2011).
[21] M.-X. Li, Z.-X. Miao, M. Shao, S.-W. Liang, and S.-R. Zhu, Inorg. Chem. **47**, 4481 (2008).
[22] M. A. Halcrow, Polyhedron **26**, 3523 (2007).
[23] Clusters of a few atoms size already show a significant broadening in XAS due to hybridization with the neighbor atoms (see e.g., Refs. [2,24,25]).
[24] P. Gambardella, S. S. Dhesi, S. Gardonio, C. Grazioli, P. Ohresser, and C. Carbone, Phys. Rev. Lett. **88**, 047202 (2002).
[25] K. Hirsch, J. T. Lau, Ph. Klar, A. Langenberg, J. Probst, J. Rittmann, M. Vogel, V. Zamudio-Bayer, T. Möller, and B. von Issendorff, J. Phys. B **42**, 154029 (2009).
[26] G. van der Laan and I. W. Kirkman, J. Phys. Condens. Matter **4**, 4189 (1992).
[27] F. Zheng, V. Perez-Dieste, J. McChesney, Y.-Y. Luk, N. L. Abbott, and F. Himpsel, Surf. Sci. **587**, L191 (2005).
[28] T. J. Regan, H. Ohldag, C. Stamm, F. Nolting, J. Lüning, J. Stöhr, and R. L. White, Phys. Rev. B **64**, 214422 (2001).
[29] We rule out that the magnetization is due to Fe clusters, as we do not observe their presence in any STM images taken at various sample locations of the very same preparation of the Fe-T4PT network. Uncoordinated Fe clusters can be further excluded by the line shape [23] of the XAS and XMCD signals and by the magnetization behavior. The magnetization of potential residual Fe clusters would have an in-plane anisotropy [30], contrary to our observed easy-axis anisotropy.
[30] P. Ohresser, N. B. Brookes, S. Padovani, F. Scheurer, and H. Bulou, Phys. Rev. B **64**, 104429 (2001).
[31] This conclusion is robust and does not depend on the assumption of an $S = 2$ high-spin state. Even stronger magnetic coupling between Fe atoms is necessary to reproduce the experimental data of Fig. 4 if $S = 1$.
[32] L. Zhou, J. Wiebe, S. Lounis, E. Vedmedenko, F. Meier, S. Blügel, P. H. Dederichs, and R. Wiesendanger, Nat. Phys. **6**, 187 (2010).
[33] N. Tsukahara, S. Shiraki, S. Itou, N. Ohta, N. Takagi, and M. Kawai, Phys. Rev. Lett. **106**, 187201 (2011).
[34] B. Fischer and M. W. Klein, Phys. Rev. B **11**, 2025 (1975).
[35] F. Reinert, G. Nicolay, S. Schmidt, D. Ehm, and S. Hüfner, Phys. Rev. B **63**, 115415 (2001).
[36] V. Bellini, G. Lorusso, A. Candini, W. Wernsdorfer, T. B. Faust, G. A. Timco, R. E. P. Winpenny, and M. Affronte, Phys. Rev. Lett. **106**, 227205 (2011).
[37] K. Inoue, and H. Iwamura, J. Am. Chem. Soc. **116**, 3173 (1994).
[38] K. Inoue, T. Hayamizu, H. Iwamura, D. Hashizume, and Y. Ohashi, J. Am. Chem. Soc. **118**, 1803 (1996).
[39] I. Horcas, R. Fernandez, J. M. Gomez-Rodriguez, J. Colchero, J. Gomez-Herrero, and A. M. Baro, Rev. Sci. Instrum. **78**, 013705 (2007).